VISUAL AMPLIFICATION OF OCULOMOTOR SIGNS FOR PARKINSONIAN PATTERNS RECOGNITION

ISAIL SALAZAR ACOSTA

UNIVERSIDAD INDUSTRIAL DE SANTANDER
FACULTAD DE INGENIERÍAS FÍSICOMECÁNICAS
ESCUELA DE INGENIERÍA DE SISTEMAS E INFORMÁTICA
BUCARAMANGA
2020

VISUAL AMPLIFICATION OF OCULOMOTOR SIGNS FOR PARKINSONIAN PATTERNS RECOGNITION

ISAIL SALAZAR ACOSTA

Research work in partial fulfillment of the requirements for the degree of:
Magíster en Ingeniería de Sistemas e Informática

Advisor:
Fabio Martínez Carrillo
Ph.D in Systems and Computer Engineering

Co-advisor:
Said David Pertuz Arroyo
Ph.D in Computer Science

UNIVERSIDAD INDUSTRIAL DE SANTANDER
FACULTAD DE INGENIERÍAS FÍSICOMECÁNICAS
ESCUELA DE INGENIERÍA DE SISTEMAS E INFORMÁTICA
BUCARAMANGA
2020

ACKNOWLEDGEMENTS

The author expresses his gratitude to the Parkinson foundation FAMPAS *(Fundación del Adulto Mayor y Parkinson Santander)* and the local elderly institution *Asilo San Rafael* for supporting the recording of the dataset proposed in this work.

This work would not have been possible without the efforts of Professor Fabio Martínez, who at every moment was contributing valuable ideas and assisting in the development of the methodology. Many thanks to him for his patience and the many hours he spent providing insight, advice, and direction.

Additional thanks to Professor Said Pertuz for his fruitful recommendations and detailed feedback, and to Dr. William Contreras for reviewing the recording protocols implemented in this work and his assistance regarding Parkinson's disease.

CONTENTS

LIST OF FIGURES

page

LIST OF TABLES

page

LIST OF ANEXOS

page

RESUMEN

TÍTULO: AMPLIFICACIÓN VISUAL DE SIGNOS ÓCULO-MOTORES PARA EL RECONOCIMIENTO DE PATRONES PARKINSONIANOS [*]

AUTOR: ISAIL SALAZAR ACOSTA [**]

PALABRAS CLAVE: ENFERMEDAD DE PARKINSON, FIJACIÓN OCULAR, PATRONES ÓCULO-MOTORES, MAGNIFICACIÓN DE MOVIMIENTO, CARACTERÍSTICAS CONVOLUCIONALES.

DESCRIPCIÓN:

Las alteraciones óculo-motoras constituyen un biomarcador prometedor para detectar y caracterizar la enfermedad de Parkinson (EP), inclusive en etapas pródromas. En la actualidad, sin embargo, solo se cuenta con el uso de dispositivos de seguimiento visual que entregan trayectorias globales y simplificadas para aproximar la compleja cinemática de la función óculo-motora. La adquisición de estas señales además suele requerir de protocolos intrusivos y sofisticados pasos de calibración. Este trabajo presenta un novedoso biomarcador de imagen para evaluar la EP mediante el modelamiento de los movimientos de fijación ocular, registrados con cámaras convencionales. En primer lugar, se realiza un proceso de magnificación de video basado en aceleración, cuyo fin es mejorar visualmente pequeños patrones relevantes de fijación en los videos capturados. Seguidamente se procede a extraer un conjunto de cortes espacio-temporales por video, los cuales son representados como mapas de características desde las primeras capas pre-entrenadas de redes neuronales convolucionales. A continuación, estos mapas se codifican eficientemente mediante matrices de covarianza para el entrenamiento de una máquina de soporte vectorial que lleva a cabo la clasificación de la enfermedad. Utilizando un conjunto de 130 videos en un estudio con 13 pacientes PD y 13 control, el enfoque propuesto alcanzó una precisión media de 95.4% y un área bajo la curva ROC de 0.984, siguiendo un esquema de validación cruzada por paciente excluido. El descriptor introducido captura adecuadamente en los ojos patrones de temblor conocidos en PD mostrando un desempeño sobresaliente.

---

[*] Trabajo de investigación

[**] Facultad de Ingenierías Físico-Mecánicas. Escuela de Ingeniería de Sistemas e Informática. Director: Fabio Martínez Carrillo, Ph.D. Codirector: Said David Pertuz Arroyo, Ph.D.

ABSTRACT

TITLE: VISUAL AMPLIFICATION OF OCULOMOTOR SIGNS FOR PARKINSONIAN PATTERNS RECOGNITION [*]

AUTHOR: ISAIL SALAZAR ACOSTA [**]

KEYWORDS: PARKINSON'S DISEASE, OCULAR FIXATION, OCULOMOTOR PATTERNS, MOTION MAGNIFICATION, CNN FEATURES.

DESCRIPTION:

Oculomotor alterations constitute a promising biomarker to detect and characterize Parkinson's disease (PD), even in prodromal stages. Currently, however, only global and simplified gaze trajectories, obtained from tracking devices, are used to approximate the complex kinematics of the oculomotor function. Besides, the acquisition of such signals often requires sophisticated calibration and intrusive settings. This work presents a novel imaging biomarker for PD assessment that models ocular fixational movements, recorded with conventional cameras. Firstly, a video acceleration magnification is performed to visually enhance small relevant fixation patterns on standard gaze video recordings. Hence, from each video are extracted a set of spatio-temporal slices, which thereafter are represented as convolutional feature maps, recovered as the first layer responses of pre-trained CNN architectures. The feature maps are then efficiently encoded by means of covariance matrices to train a support vector machine and perform the disease classification. From a set of 130 recordings in a study of 13 PD patients and 13 age-matched controls, the proposed approach achieved an average accuracy of 95.4% and an area under the ROC curve of 0.984, following a leave-one-patient-out cross-validation scheme. The introduced imaging-based descriptor is able to properly capture known disease tremor patterns in the eyes, since PD classification performance is outstanding when augmented motion frequencies were fixed within tremor-related pathological ranges.

---

[*] Research work

[**] Facultad de Ingenierías Físico-Mecánicas. Escuela de Ingeniería de Sistemas e Informática. Advisor: Fabio Martínez Carrillo, Ph.D. Co-advisor: Said David Pertuz Arroyo, Ph.D.

INTRODUCTION

Parkinson's disease (PD) is the second most common neurodegenerative disorder in the world. Reported incidence indicates a typical affectation of 2–3% of the population older than 65 years old [1], with an expectation of doubling by 2030. PD symptoms are mainly motor, involving progressive and involuntary alterations over the mobility of different body segments, such as tremor, bradykinesia (slow movement) and stiffness. These physical impairments are the direct consequence of a gradual decline in dopamine levels [2], a biomolecule the brain uses to conduct neurotransmission of motor commands.

In spite of recent advances in neuroimaging and genetics, the loss of dopamine-secreting cells remains poorly understood, resulting in diagnostic procedures that rely on conspicuous motor alterations. In clinical practice, such procedures carry out specific observational tests, like the Unified Parkinson's Disease Rating Scale (UPDRS) and the Hoehn-Yahr Scale, that coarsely correlate the patients' motor behavior with different disease stages [3]. This evaluation is however prone to bias and subjectivity due to the high interpersonal variability of patients' motion and the particular physician's experience and perception [4]. Hence, quantitative and reproducible

---

1 POEWE, Werner , *et al.* "Parkinson disease". In: *Nature reviews Disease primers* 3 (2017), p. 17013.

2 JANKOVIC, Joseph. "Parkinson's disease: clinical features and diagnosis". In: *Journal of neurology, neurosurgery & psychiatry* 79.4 (2008), pp. 368–376.

3 VENUTO, Charles S, *et al.* "A review of disease progression models of Parkinson's disease and applications in clinical trials". In: *Movement Disorders* 31.7 (2016), pp. 947–956.

4 RIZZO, Giovanni, *et al.* "Accuracy of clinical diagnosis of Parkinson disease A systematic review and meta-analysis". In: *Neurology* 86.6 (2016), pp. 566–576.

models are currently in demand to objectively support PD assessment. Also, such models should have a special emphasis in the early stages of the disease, where the motor impairment degree is very subtle. In fact, diagnostic error rates on early stages have been quantified above 24% even in specialized centres [1].

Machine learning (ML) and pattern recognition methods have allowed to improve the diagnostic and monitoring paradigm of PD by modeling several kinematic symptoms [5]. Specifically, relevant works have reported significant discrimination between PD and healthy patterns by applying supervised ML algorithms over on-body sensor signals [6] [7]. Other well-performing approaches have considered the use of video information in deep learning architectures [8] [9]. These schemes have mainly worked on classification and recognition of PD gait and tremor behaviors, focusing on upper and lower limbs. However, limb motor symptoms generally appear in middle and advanced disease stages, after the loss of 50% of dopamine-secreting cells [10].

---

[5] BELIĆ, Minja, *et al.* "Artificial intelligence for assisting diagnostics and assessment of Parkinson's disease–A review". In: *Clinical neurology and neurosurgery* (2019), p. 105442.

[6] CARAMIA, Carlotta, *et al.* "IMU-Based Classification of Parkinson's Disease From Gait: A Sensitivity Analysis on Sensor Location and Feature Selection". In: *IEEE journal of biomedical and health informatics* 22.6 (2018), pp. 1765–1774.

[7] ABDULHAY, Enas, *et al.* "Gait and tremor investigation using machine learning techniques for the diagnosis of Parkinson disease". In: *Future Generation Computer Systems* 83 (2018), pp. 366–373.

[8] HU, Kun, *et al.* "Vision-based freezing of gait detection with anatomic patch based representation". In: *Asian Conference on Computer Vision*. Springer. 2018, pp. 564–576.

[9] AJAY, Jerry, *et al.* "A pervasive and sensor-free deep learning system for Parkinsonian gait analysis". In: *2018 IEEE EMBS International Conference on Biomedical & Health Informatics (BHI)*. IEEE. 2018, pp. 108–111.

[10] SALAT, David, *et al.* "Challenges of modifying disease progression in prediagnostic Parkinson's disease". In: *The Lancet Neurology* 15.6 (2016), pp. 637–648.

The eye movements have emerged as a potential and very promising PD biomarker with strong diagnostic confidence at the disease onset. For instance, patients with rapid eye movement disturbances during sleep have shown a high risk for developing PD [11], reporting conversion rates between 15% and 40% over 2-5 years and up to 90% with longer follow-up beyond 10 years. Furthermore, several works have found specific and subtle abnormalities on a variety of eye movements in typical visual tasks performed by PD patients [12] ,[13] ,[14]. The described alterations point out a drastic association between the oculomotor function and the neurodegenerative process of the brain. A relation that can be anatomically explained by studying the multiple brain structures and neural circuits involved in the oculomotor control [15]. For this reason, it is fundamental to detect and quantify oculomotor disturbances, especially those that have been confirmed in large cohorts of PD patients at different stages. In particular, the work of Gitchel et al. [16] demonstrated the presence of unstable fixations on 112 patients with PD and in 2 out of 60 asymptomatic control subjects.

---

[11] IRANZO, Alex; SANTAMARIA, Joan, and TOLOSA, Eduardo. "Idiopathic rapid eye movement sleep behaviour disorder: diagnosis, management, and the need for neuroprotective interventions". In: *The Lancet Neurology* 15.4 (2016), pp. 405–419.

[12] GORGES, Martin, *et al.* "The association between alterations of eye movement control and cerebral intrinsic functional connectivity in Parkinson's disease". In: *Brain imaging and behavior* 10.1 (2016), pp. 79–91.

[13] EKKER, Merel S, *et al.* "Ocular and visual disorders in Parkinson's disease: Common but frequently overlooked". In: *Parkinsonism & related disorders* 40 (2017), pp. 1–10.

[14] TURCANO, Pierpaolo, *et al.* "Early ophthalmologic features of Parkinson's disease: a review of preceding clinical and diagnostic markers". In: *Journal of neurology* (2018), pp. 1–9.

[15] GOLDBERG, M. E and WALKER, M. F. "The control of gaze". In: *Principles of Neural Science*. Ed. by KANDEL, Eric R., *et al.* 5th. USA: New York: McGraw-Hill, 2013, pp. 894–916.

[16] GITCHEL, George T; WETZEL, Paul A, and BARON, Mark S. "Pervasive ocular tremor in patients with Parkinson disease". In: *Archives of neurology* 69.8 (2012), pp. 1011–1017.

Figure 1. Ocular fixation comparison of a PD-diagnosed patient and a healthy control subject. Motion-magnified slices from eye videos show a clear improvement in the visual differentiation of both classes. (a) PD sequence where the magnification process enhances an oscillatory fixational instability. (b) Control sequence where no particular oculomotor pattern is depicted.

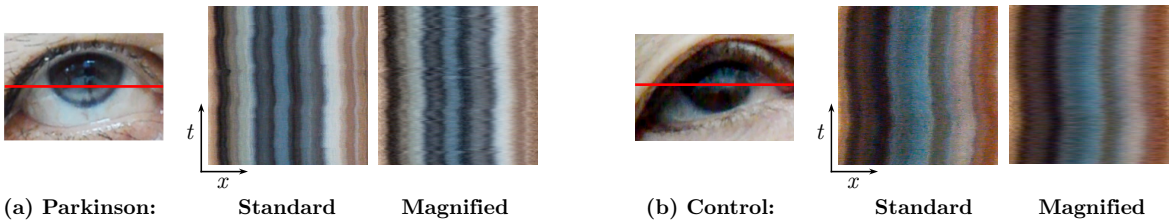

(a) Parkinson: Standard Magnified (b) Control: Standard Magnified

Incidentally, both control subjects evolved to clinical PD at 3 years of follow-up [17]. Nevertheless, a main drawback of the majority of oculomotor research lies on the utilization of video-oculography (VOG) protocols [18]. VOG recordings present limitations in that they only depict global and simplified trajectories of the whole eye motion field, and are difficult to set up and calibrate. Besides, the instrumentation usually requires contact with the entire area around the eyes, thus affecting the natural visual gesture.

This paper introduces a novel strategy to reveal and quantify fixational eye micromovements from conventionally captured videos. Such description is achieved by extracting temporal video slices that spatially project eye motion. First, small fixation patterns are enhanced by means of a video acceleration magnification. As shown in Figure 1, magnified slices can better portray the oscillatory fixational pat-

---

[17] GITCHEL, George T, *et al.* "Experimental support that ocular tremor in Parkinson's disease does not originate from head movement". In: *Parkinsonism & related disorders* 20.7 (2014), pp. 743–747.

[18] LARRAZABAL, AJ; CENA, CE García, and MARTÍNEZ, CE. "Video-oculography eye tracking towards clinical applications: A review". In: *Computers in biology and medicine* 108 (2019), pp. 57 –66.

terns that visually differentiate between control and PD eye motion. Subsequently, a dense slice representation is obtained by computing early layer responses in relevant deep learning architectures. These responses correspond to pre-learned and multi-channel filter outputs that are compactly codified as a channel-wise covariance matrix. Major information energy is captured according to an eigenvalue decomposition. Then, the resulting covariance is mapped to a previously trained support vector machine in order to classify the disease given a certain set of eye slices.

Experiments were performed over 130 eye sequences from 13 PD-diagnosed patients and 13 age-matched control subjects, through a leave-one-patient-out cross-validation scheme. The achieved results show high effectiveness to codify fixation motility and to discriminate between both classes. Three main contributions are:

- A novel computational framework to characterize ocular fixation, resulting in an imaging biomarker for the quantitative assessment of Parkinson's disease while avoiding complex protocols and sophisticated devices.
- A video dataset of relevant eye movements in typical visual tasks for control and parkinsonian populations, from a simple and comfortable recording protocol with a conventional camera.
- An extensive evaluation to demonstrate that video magnification can be a powerful tool for improving performance in parkinsonian oculomotor assessment while providing a visual enhancement of tenuous abnormalities.

The proposed approach in this research work could potentially provide support and assistance on diagnostic procedures and follow-up of PD progression. Particularly, this methodology constitutes a promising development for the evaluation of parkinsonian oculomotor patterns in practical scenarios, with prospect application on early

stages of the disease, where the most effective treatment therapies can be formulated.

1. PARKINSONIAN OCULOMOTOR ANALYSIS

Recently, oculomotor patterns have been evidenced as a highly relevant biomarker to detect and characterize PD, even in prodromal disease stages [13, 14, 19]. The oculomotor function depends on a large part of the human brain, including several cortical and subcortical areas (e.g., the brainstem, cerebellum, and basal ganglia) [15]. Hence, neurodegenerative brain changes, involved during PD progression, can be sensed from the acute sensitivity of eye motion. Fixational eye motion, in particular, represents a type of ocular motility that have been quantified in a relatively large population of PD patients, including novo untreated patients and healthy controls that eventually developed the disease [16, 20, 17].

Ocular fixation is defined as the faculty to stabilize the visual gaze at a given location, e.g., on a stationary object of interest, while the head is relatively kept in fixed position. In the study of Gitchel et al. [16], it was found the presence of a persistent ocular micro-tremor on 112 PD patients during gaze fixations. This alteration was characterized as an oscillatory pattern with a mean fundamental frequency of 5.7 $\pm$ 1.5 Hz and average magnitudes of 0.27º and 0.33º in the horizontal and vertical planes, respectively. This motion is very subtle and almost imperceptible. In a second study, it was additionally evaluated the independence of this pattern with respect to head movements [17], facing with an alternative hypothesis that explained fixational

---

[19] LAL, Vivek and TRUONG, Daniel. "Eye movement abnormalities in movement disorders". In: *Clinical Parkinsonism Related Disorders* 1 (2019), pp. 54 –63.

[20] ARCHIBALD, Neil K, *et al.* "Visual exploration in Parkinson's disease and Parkinson's disease dementia". In: *Brain* 136.3 (2013), pp. 739–750.

oculomotor disturbances as merely vestibular-ocular reflex responses [21].

Further PD oculomotor studies have analyzed different kinematic abnormalities in other types of eye movements. In saccades, for instance, the quick movement of both eyes between two fixation targets, there have been reported decreasing amplitudes (hypometric steps) and increasing latencies [12]. The antisaccadic task has also been investigated, where the eyes move away from the second fixation target, reflecting positional errors and more severely prolonged latencies [22]. Another commonly evaluated oculomotor type corresponds to the close following of a moving object, known as smooth pursuit eye movement, which is described in PD by saccadic interruptions and low pursuit gain (the ratio between peak eye velocity and peak target velocity) [23]. Finally, in vergence eye movements, where the eyes rotate towards (convergence) or away (divergence) from each other according to a target moving closer by o farther away, are reported impairments in both direction and velocity that often cause blurred vision in PD patients [24].

Some works in the computer science community have then explored these findings and have proposed statistical and learning-based approaches to quantitatively predict parkinsonian progression and diagnosis. For instance, the work presented in

---

[21] KASKI, Diego, *et al.* "Ocular tremor in Parkinson's disease is due to head oscillation". In: *Movement Disorders* 28.4 (2013), pp. 534–537.

[22] EWENCZYK, Claire, *et al.* "Antisaccades in Parkinson disease: a new marker of postural control?" In: *Neurology* 88.9 (2017), pp. 853–861.

[23] FUKUSHIMA, Kikuro , *et al.* "Impaired smooth-pursuit in Parkinson's disease: normal cue-information memory, but dysfunction of extra-retinal mechanisms for pursuit preparation and execution". In: *Physiological reports* 3.3 (2015), e12361.

[24] HANUŠKA, Jaromír, *et al.* "Fast vergence eye movements are disrupted in Parkinson's disease: A video-oculography study". In: *Parkinsonism & related disorders* 21.7 (2015), pp. 797–799.

[25] evaluated saccadic recordings of 94 PD patients, by applying random forest classifiers in order to predict the individual UPDRS scores and Levadopa dosages (most common treatment drug of PD) of the patients. Another approach [26] implements a binary logistic regression model over a combination of saccadic, smooth pursuit and fixation parameters, in a case-control evaluation of 37 PD patients and 39 controls. And very recently, in a compact study with 11 PD patients [27], decision tree algorithms were trained on antisaccadic metrics to obtain predictions of the UPDRS patient scores. A previous version of such study also evaluated saccades and smooth pursuit movements by using rough set theory [28].

All of the previously mentioned studies rely on video-oculography (VOG) monitoring schemes [29]. These VOG setups generally employ specialized infrared cameras of high spatial and temporal resolutions, and offer reliable and noise-free recordings of eye movement. Nonetheless, the registered signals are limited to global eye-tracking relationships and the quantification of primary orders for the description of eye kinematic parameters. Additionally, the required equipment can become intrusive by

---

[25] SZYMAŃSKI, Artur, *et al.* "Building Intelligent Classifiers for Doctor-Independent Parkinson's Disease Treatments". In: *Conference of Information Technologies in Biomedicine*. Springer. 2016, pp. 267–276.

[26] ZHANG, Yu, *et al.* "Oculomotor Performances Are Associated With Motor and Non-motor Symptoms in Parkinson's Disease". In: *Frontiers in neurology* 9 (2018), p. 960.

[27] SLEDZIANOWSKI, Albert, *et al.* "Measurements of Antisaccades Parameters Can Improve the Prediction of Parkinson's Disease Progression". In: *Asian Conference on Intelligent Information and Database Systems*. Springer. 2019, pp. 602–614.

[28] KUBIS, Anna; SZYMAŃSKI, Artur, and PRZYBYSZEWSKI, Andrzej W. "Fuzzy Rough sets theory applied to parameters of eye movements can help to predict effects of different treatments in Parkinson's patients". In: *International Conference on Pattern Recognition and Machine Intelligence*. Springer. 2015, pp. 325–334.

[29] KHOSLA, Ajit and KIM, Dongsoo. *Optical Imaging Devices: New Technologies and Applications*. CRC Press, 2015.

covering the entire eye region, is expensive, and require calibration and configuration procedures. In order to tackle these issues, alternatives for oculomotor examination that only use common video sequences have been recently introduced [30] [,31] [,32]. Such strategies model spatio-temporal pixel relationships based on diverse computer vision algorithms, under semi-controlled conditions and without complex requirements regarding the devices used.

Despite the advances in developing video descriptors for oculomotor quantification, existing methods are restricted to capture saccadic eye movements, described as large iris displacements in different visual exploration tasks. These approaches require greater efforts to describe the tiny and subtle oculomotor behaviors in other varieties of eye movements. Additionally, it should be considered that these movements can be masked by unavoidable comparatively larger movements of the patient's head. In this way, oculomotor patterns potentially descriptive for PD detection and prognosis, could be better assessed.

---

[30] TRUJILLO, David, *et al.* "A characterization of Parkinson's disease by describing the visual field motion during gait". In: *11th International Symposium on Medical Information Processing and Analysis*. Vol. 9681. SPIE (2015).

[31] ADHIKARI, Sam and STARK, David E. "Video-based eye tracking for neuropsychiatric assessment". In: *Annals of the New York Academy of Sciences* 1387.1 (2017), pp. 145–152.

[32] LAI, Hsin-Yu, *et al.* "Enabling Saccade Latency Measurements with Consumer-Grade Cameras". In: *2018 25th IEEE International Conference on Image Processing (ICIP)*. IEEE. 2018, pp. 3169–3173.

2. RESEARCH PROBLEM

Current acquisition systems for quantitative oculomotor examination do not represent the whole eye motion field and its intrinsic deformations. In addition, since the equipment is expensive, difficult to set up and calibrate, it is necessarily limited to laboratory research and restrictive protocols. Other alternatives perform the oculomotor evaluation on video by using consumer-grade cameras. However, they do not consider subtle oculomotor alterations that prove to be of great importance for assisting early PD diagnosis and tracking disease progression.

Research Question: How to describe subtle oculomotor patterns registered on video that may be associated with the Parkinson's disease?

General Objective

To propose a quantitative description of ocular micro-motion in video for diagnostic support of Parkinson's disease.

Specific Objectives

- To build a video dataset of relevant oculomotor patterns in parkinsonian and control populations.
- To visually amplify eye motion through video magnification techniques.
- To quantitatively describe oculomotor behavior on standard and magnified videos.
- To evaluate the performance of the proposed approach in the recorded video dataset.

3. PROPOSED APPROACH

The proposed pipeline is illustrated in Figure 2. Three fundamental steps are considered and will be detailed in the following sections.

3.1. VIDEO ACCELERATION MAGNIFICATION

A remarkable fact of PD fixations is their abnormal and subtle oscillatory behavior which has been strongly correlated with Parkinson's disease [16, 17]. Nevertheless, the quantification of these involuntary eye micro-movements constitutes a major limitation for fixational PD motion analysis. An additional challenge underlies on decoding the tiny eye displacement when masked on comparatively larger head motion. This work hence starts by performing an optical spatio-temporal amplification over fixation sequences. A set of specific motion-related frequencies were amplified by using a video acceleration magnification approach [33], which allows to amplify subtle

[33] ZHANG, Yichao; PINTEA, Silvia L., and VAN GEMERT, Jan C. "Video Acceleration Magnification". In: *Computer Vision and Pattern Recognition*. 2017.

Figure 2. Pipeline of the proposed approach. (a) Video acceleration magnification (section 3.1). (b) A convolutional fixation representation (section 3.2). (c) Recognizing PD from a compact fixational descriptor (section 3.3).

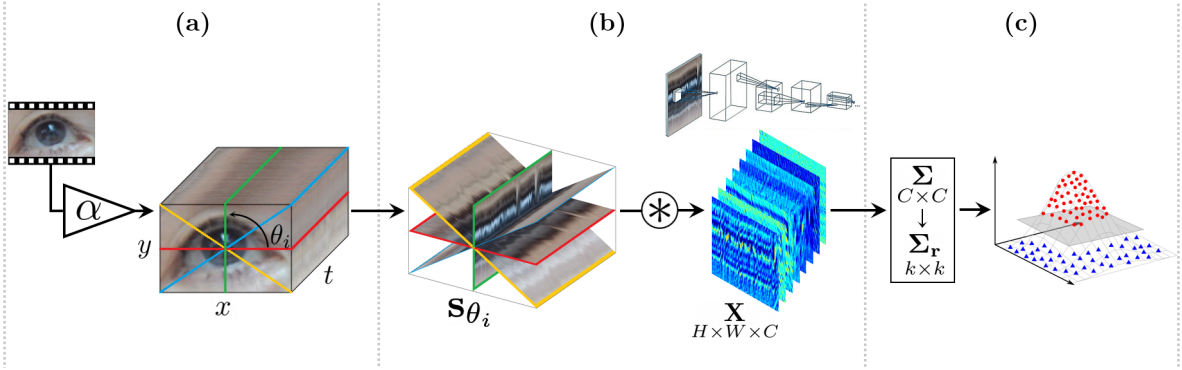

motion (eye fixations) even in the presence of large motion (head). The acceleration magnification works by analyzing local motion of video pixels, a derivation that can be computed from spatially localized phase information [34]:

$$I(\mathbf{x}, t) * \Omega_{w,\theta} = A_{w,\theta}(\mathbf{x}, t)\, e^{i\,\Phi_{w,\theta}(\mathbf{x},t)}\ , \tag{1}$$

where $I(\mathbf{x}, t)$ represents a pixel signal at coordinate $\mathbf{x} = [x, y]$ and $\Omega_{w,\theta}$ is a complex-valued steerable pyramid [35], with w spatial frequency bands and θ orientations.
The local phase is then extracted and decomposed into a second-order Taylor series around t:

$$\Phi_{w,\theta}(\mathbf{x}, t+1) \approx\ \Phi_{w,\theta}(\mathbf{x}, t) + \frac{\partial \Phi_{w,\theta}(\mathbf{x},t)}{\partial t} + \frac{1}{2}\frac{\partial^2 \Phi_{w,\theta}(\mathbf{x},t)}{\partial t^2} \tag{2}$$

The first-order term in Eq. 2 represents linear magnitude changes on velocity, while the second-order term measures the deviation of motion change, i.e., acceleration. Previous magnification methods focused on amplifying velocity [36] ,[37]. In this case, considering that velocity quantifies all motion changes without discriminating between large or small ones, then, for amplifying small motion in the presence of large motion, the acceleration can be used. This fact assumes, from the acceleration point of view, that large motions are approximately linear at the temporal scale of small motion. Therefore, all linear motion is disregarded from the analysis. For doing so, only

---

[34] FLEET, David J and JEPSON, Allan D. "Computation of component image velocity from local phase information". In: *International journal of computer vision* 5.1 (1990), pp. 77–104.

[35] PORTILLA, Javier and SIMONCELLI, Eero P. "A parametric texture model based on joint statistics of complex wavelet coefficients". In: *International journal of computer vision* 40.1 (2000), pp. 49–70.

[36] WU, Hao-Yu, *et al.* "Eulerian Video Magnification for Revealing Subtle Changes in the World". In: *ACM Transactions on Graphics (Proc. SIGGRAPH 2012)* 31.4 (2012).

[37] WADHWA, Neal, *et al.* "Phase-based video motion processing". In: *ACM Transactions on Graphics (TOG)* 32.4 (2013), p. 80.

the second-order phase derivative is taken into account, which is obtained through the Laplacian of Gaussian operator:

$$\Phi''_{w,\theta}(\mathbf{x},t) = \frac{\partial^2 \Phi_{w,\theta}(\mathbf{x},t)}{\partial t^2} = \Phi_{w,\theta}(\mathbf{x},t) * \frac{\partial^2 G_\sigma(\mathbf{x},t)}{\partial t^2} \ , \tag{3}$$

where σ is the Gaussian filter standard deviation.

Then, phases are amplified as follows:

$$\hat{\Phi}_{w,\theta}(\mathbf{x},t) = \Phi_{w,\theta}(\mathbf{x},t) \ + \ \alpha \ \Phi''_{w,\theta}(\mathbf{x},t) \ , \tag{4}$$

where α is the magnification factor, which amplifies second-order changes at a temporal frequency $f = \frac{f_r}{8\pi\sqrt{2}\,\sigma}$, with $f_r =$ video frame rate.

3.2. A CONVOLUTIONAL FIXATION REPRESENTATION

The resulting amplified video $\hat{I}(\mathbf{x},t)$ is split-up into a set of spatio-temporal slices $\mathrm{S}_\theta = \{\mathrm{s}_{\theta_1}, \mathrm{s}_{\theta_2}, \quad \ldots, \mathrm{s}_{\theta_N}\}$ at N orientations. In this way, each slice records temporal tremor signals together with natural eye motion signals. To compute these slices, different radial directions on the spatial xy-plane were used as a reference along time. A typical radial configuration is illustrated in Figure 3. Eye slices then capture small eye iris displacements and herein constitute an ideal source of information to analyze small ocular movements.

Figure 3. Spatio-temporal video slices. At different slice directions, relevant cues in fixation recordings can be captured.

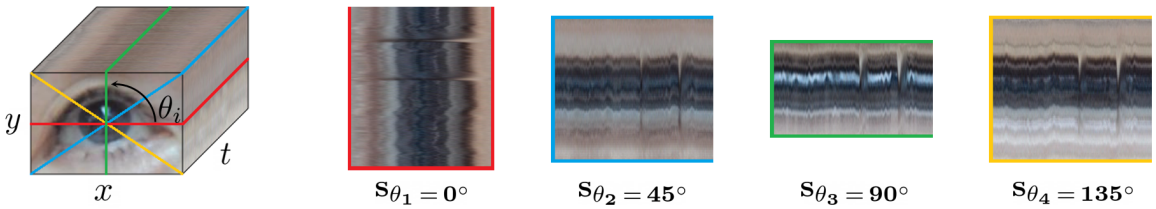

A slice feature decomposition is applied to analyze hidden parkinsonian tremor patterns involved in ocular fixation signals. Each slice s_{θ_i} is represented as a bank of separated band responses of multiple spatial frequency filters. To this end, slices S_θ are mapped onto the first layers of known and pre-trained deep convolutional frameworks, which have been implemented for a general natural image classification problem. In brief, such architectures progressively compute linear transformations, followed by contractive nonlinearities, projecting information on a set of C learned filters $\mathbf{\Psi}^j = \{\boldsymbol{\psi}_1^j, \boldsymbol{\psi}_2^j, \ldots, \boldsymbol{\psi}_C^j\}$ at a given layer j. Hence, each eye slice s_{θ_i} is filtered by a particular $\mathbf{\Psi}^j$ set, obtaining a convolutional feature representation:

$$\mathbf{X}^j = \Big|\Big|_{c=1}^{C} \mathrm{s}_{\theta_i} * \boldsymbol{\psi}_c^j = \Big|\Big|_{c=1}^{C} \boldsymbol{\chi}_c^j \ , \tag{5}$$

with $||$ representing concatenation and $\boldsymbol{\chi}_c^j$ as each independent feature channel.

The discovery of an efficient representation that captures key visual concepts on particular domains has been an open problem on computer vision. Classical representations such as the wavelets have been effective on several domains, but requiring specific analysis about the nature of signals and an exhaustive tuning to represent objects of interest. In contrast, representations based on learned convolutional schemes, which are originally optimized for object classification, have turned out successful for other generic tasks [38] ,[39]. These representations namely use the last

---

[38] SHARIF RAZAVIAN, Ali, *et al.* "CNN features off-the-shelf: an astounding baseline for recognition". In: *Proceedings of the IEEE conference on computer vision and pattern recognition workshops*. 2014, pp. 806–813.

[39] DONAHUE, Jeff, *et al.* "Decaf: A deep convolutional activation feature for generic visual recognition". In: *International conference on machine learning*. 2014, pp. 647–655.

fully connected vectors as input on conventional non-linear classifiers. Such vectors capture salient semantic concepts of complex visual objects. In this work, the salient parkinsonian fixation patterns are represented as primitive signals spatially embedded in the background. Therefore, the use of first layers that decompose primitive and low-level features of slice signals is an optimal and sufficient representation.

3.3. RECOGNIZING PD FROM A COMPACT FIXATIONAL DESCRIPTOR

The feature representation $\mathbf{X} \in \mathbb{R}^{H \times W \times C}$ for each slice $\mathbf{s}_\theta$ is composed by C filter responses $\boldsymbol{\chi}_c$ with dimensions $H \times W$. This information is nevertheless redundant on spatial background, since parkinsonian fixation patterns present alterations of oscillatory and periodic nature. For this reason, a channel-wise covariance is herein computed from feature maps, providing a compact measure of relationship between the different feature channels. For doing so, each $\boldsymbol{\chi}_c$ is first vectorized, reshaping $\mathbf{X}$ to $HW \times C$, i.e., $\mathbf{X}$ is now a matrix of C-dimensional feature vectors. From here, the feature covariance calculation can be expressed as:

$$\boldsymbol{\Sigma} = \tfrac{1}{HW}[\mathbf{X} - \mu(\mathbf{X})][\mathbf{X} - \mu(\mathbf{X})]^T \ , \tag{6}$$

with $\mu(\mathbf{X})$ as the mean $1 \times C$ feature vector repeated HW times vertically.
The covariance $\boldsymbol{\Sigma} \in \mathbb{R}^{C \times C}$ then describes a second statistical moment on the whole feature space, that compactly summarizes the fixational motion representation from each particular eye slice. From a spectral matrix analysis, $\boldsymbol{\Sigma} = \mathbf{V}\boldsymbol{\Lambda}\mathbf{V}^{\mathbf{T}}$, $\boldsymbol{\Lambda}$ eigenvalues and $\mathbf{V}$ eigenvectors, only information related to the k major eigenvalues is preserved, where the energy of $\boldsymbol{\Sigma}$ is fully concentrated. In this way, a new reduced covariance $\boldsymbol{\Sigma}_\mathbf{r}$ that captures the most variability of the C feature channels is computed as:

$$\underset{k \times k}{\boldsymbol{\Sigma}_\mathbf{r}} = \mathbf{W}^\mathbf{T}\boldsymbol{\Sigma}\,\mathbf{W} \ , \tag{7}$$

where $\mathbf{W} \in \mathbb{R}^{C \times k}$ is the reduced eigenvector matrix of $\mathbf{\Sigma}$ with $k < C$.
Due to the semi-definite and positive properties of covariance matrices, they exist on a semi-spherical Riemannian space. This fact limits the application of classic machine learning approaches that assume Euclidean structured data. Thus, $\mathbf{\Sigma_r}$ is projected onto the Euclidean space by taking the matrix logarithm of $\mathbf{\Sigma_r}$. That is,

$$\log(\mathbf{\Sigma_r}) = \mathbf{V_r} \log(\mathbf{\Lambda_r}) \mathbf{V_r^T} \ , \tag{8}$$

where $\mathbf{V_r}$ are the eigenvectors of $\mathbf{\Sigma_r}$ and $\log(\mathbf{\Lambda_r})$ the corresponding logarithmic eigenvalues.

The reduced covariance in Eq. (8) represents the fixational motion descriptor to be fed into a machine learning algorithm in order to obtain a prediction of Parkinson's disease, under a supervised learning scheme. In this work, a support vector machine (SVM) is selected as supervised model due to its demonstrated capability at defining non-linear boundaries between classes. Also, SMVs have widely reported proper performance on high dimensional data with low computational complexity. In general, an SVM models an optimization problem by using Lagrangian multipliers to find the best hyperplanes that separate training data, i.e., maximizing margin distance between classes. Since covariance descriptors could face non-linear boundaries, a mapping function (kernel) is applied to map the original descriptor into a higher dimensional space, and therefore finding best boundaries that separate parkinsonian from control covariances. In that way, the classical yet powerful Radial Basis

Function (RBF) kernel is utilized [40]:

$$K = \exp\left(-\gamma \,||\log(\mathbf{\Sigma_r})_i - \log(\mathbf{\Sigma_r})_j||^2\right) \ , \tag{9}$$

where $\gamma > 0$ is a kernel parameter to be tuned.

[40] CHANG, Chih-Chung and LIN, Chih-Jen. "LIBSVM: A library for support vector machines". In: *ACM Transactions on Intelligent Systems and Technology* 2 (3 2011), 27:1–27:27.

4. EXPERIMENTAL SETUP

4.1. PROPOSED DATASET

In this work was proposed and implemented a protocol to record fixational eye movements on PD-diagnosed and control patients. Participants were invited to observe and follow a white circular stimulus projected on a 32-inch screen with a black background, as shown in Figure 4 (a). A conventional camera, Nikon D3200, with a spatial resolution of 1280 $\times$ 720 pixels and a temporal resolution of 60 fps was fixed in front of the subjects to capture their upper face region. Individual eyes were manually cropped (210 $\times$ 140 pixels) to obtain the sequences of interest. A total of 13 PD patients (average age of 72.3 $\pm$ 7.4) and 13 control subjects (average age of 72.2 $\pm$ 6.1) were captured and analyzed for validation of the proposed approach. Gender distribution for the PD group was {F=3, M=10}, and for the control group was {F=8, M=5}. Confounding effects are considered in section 5.1. PD patients were taking their usual prescribed medication (Levadopa mainly), and were evaluated in second (5 patients), third (6 patients) and fourth (2 patients) stage of the disease by a physician using standard protocols of the Hoehn-Yahr scale [41].

The recorded sequences contain three principal types of eye movements: fixations, saccades and smooth pursuit movements. Fixations were analyzed between smooth pursuit and random saccades. A sample stimuli sequence is illustrated in Figure 4 (b). From this set of visual tasks is obtained a single eye fixation sample. In the same way, another 4 samples were obtained for a total of 5 fixation samples per

[41] GOETZ, Christopher G, *et al.* "Movement Disorder Society Task Force report on the Hoehn and Yahr staging scale: status and recommendations the Movement Disorder Society Task Force on rating scales for Parkinson's disease". In: *Movement disorders* 19.9 (2004), pp. 1020–1028.

Figure 4. Recording protocol of eye movements. (a) Scenario configuration. (b) Sample stimuli sequence for one eye-recording round. The dot stimulus induces ocular fixations in the middle of other relevant visual tasks (smooth pursuit and random saccades). For the evaluation step in this work, only the central 5 seconds of the total fixation period were taken into account.

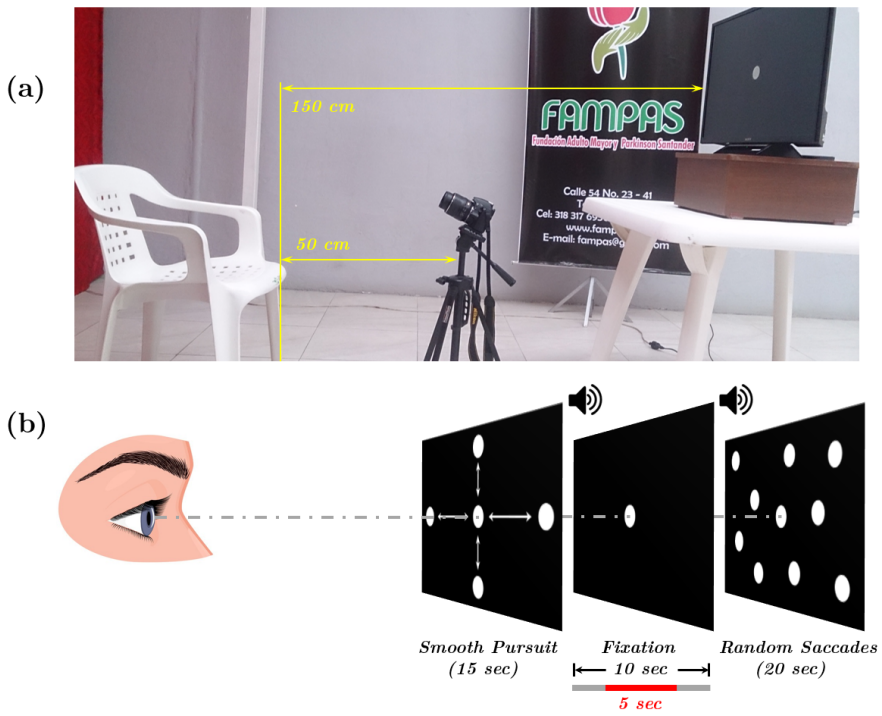

person, with duration of 5 seconds each. Over the 26 participants, this gives a total dataset of 130 eye fixation sequences. Details about the other stimuli sequences and recordings are presented in Anexo B.

This study was approved by the Ethics Committee of the Universidad Industrial de Santander in Bucaramanga – Colombia, in accordance with international ethical standards such as the Helsinki Declaration and the Belmont Report. Participants were recruited from the local Parkinson foundation FAMPAS *(Fundación del Adulto Mayor y Parkinson Santander)* and the local elderly institution *Asilo San Rafael*. Written informed consent was obtained for every participant (see Anexo C for a scanned copy with the assent of the ethics committee).

Figure 5. Visual effect by using different magnification factors. As observed, the magnification stand out micro-tremor patterns that could be crucial to characterize Parkinson's disease.

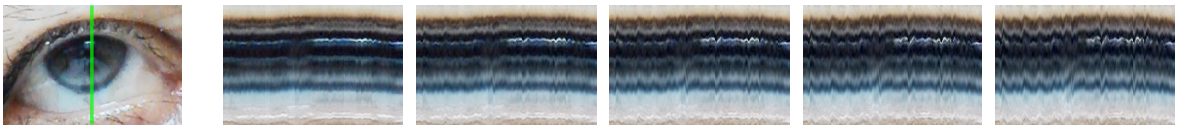

4.2. MAGNIFICATION PARAMETERS

In this work, two different configurations were considered: standard raw videos and magnified videos. Figure 1 illustrates standard and magnified ocular fixational motion for sample PD and control subjects. Magnified PD slices show well-defined amplitudes of slight oscillatory motility at frequencies around 6 Hz, the selected motion-magnified frequency. A quantitative analysis of the effect of different magnification frequencies is presented in chapter 5. Regarding the magnification factor, a visually reasonable value to emphasize this subtle oscillatory pattern was found to be $\alpha = 15$, as illustrated in the spatio-temporal comparison of Figure 5.

4.3. CNN FEATURE MAPS

Five different pre-trained CNN architectures were studied and independently used for eye slice dense representation. Each of the selected architectures was previously trained by their authors on the ImageNet dataset (a total training set of around 1.2 million samples) [42]. The summarized description of the studied deep architectures, focused on a specific first layer herein used for representation, is described as follows:

---

[42] DENG, Jia, *et al.* "ImageNet: A large-scale hierarchical image database". In: *2009 IEEE conference on computer vision and pattern recognition*. IEEE. 2009, pp. 248–255.

- **VGG-19** [43] is a classical CNN architecture with a total of 19 layers. For low-level representation purposes, this work considered the first block pooling layer with a total of $C = 64$ filter channels, and responses of size $W = 112 \times H = 112$.

- **ResNet-101** [44] is a deep net that includes identity residual mappings as recursive inputs on superior layers throughout shortcut connections, to address the vanishing gradient problem of training iterations. A feature representation was herein obtained from the first block pooling layer ($C = 64$, $W = 112 \times H = 112$).

- **Inception-ResNet-v2** [45] is one of the most recent approaches that combines the inception blocks, i.e., multiple sub-networks that learn independently with residual connections. In such way, this net allows optimal learning rates and thus higher training speeds. The third block ReLu layer responses of $C = 64$ and $W = 147 \times H = 147$ were used as feature representation.

- **Xception** [46] is a CNN that presents an alternative inception block formulation, using depth-wise separable convolutions, and achieving performance gains. Feature maps of $C = 64$ and $W = 147 \times H = 147$ were obtained from the second ReLu layer of the first CNN block.

---

[43] SIMONYAN, Karen and ZISSERMAN, Andrew. "Very deep convolutional networks for large-scale image recognition". In: *arXiv preprint arXiv:1409.1556* (2014).

[44] HE, Kaiming, *et al.* "Deep residual learning for image recognition". In: *Proceedings of the IEEE conference on computer vision and pattern recognition*. 2016, pp. 770–778.

[45] SZEGEDY, Christian, *et al.* "Inception-v4, inception-resnet and the impact of residual connections on learning". In: *Thirty-First AAAI Conference on Artificial Intelligence*. 2017.

[46] CHOLLET, François. "Xception: Deep learning with depthwise separable convolutions". In: *Proceedings of the IEEE conference on computer vision and pattern recognition*. 2017, pp. 1251–1258.

Figure 6. Sample filter responses from each CNN architecture. In general, selected layers exhibit a high response rate to the small local slice patterns, such as lines, edges, and corners, that are markedly accentuated by the magnification process. This representation can thus provide a suitable feature map for the depicted fixational cues.

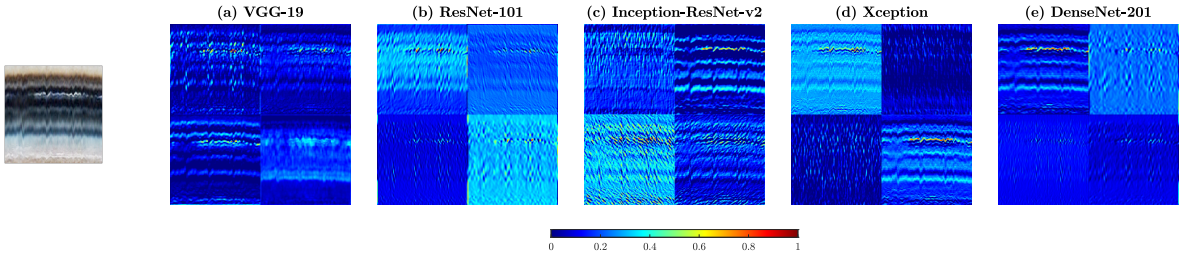

- **DenseNet-201** [47] is a densely interconnected architecture that introduces direct connections between layers in a feed-forward fashion, strengthening feature reuse and propagation, and reducing number of parameters. Convolutional features for this net were obtained from the first block ReLu layer ($C = 64$, $W = 112 \times H = 112$).

For illustration, Figure 6 shows sample responses of the utilized deep architectures for a given input eye slice, which in this case corresponds to a magnified parkinsonian slice.

After the slices (raw or magnified) were mapped to the CNN architectures, a very compact covariance descriptor was computed by using the minimal number of eigenvalues that explain about 95% of the total channel-wise feature variability in each feature representation (as described in section 3.3). Figure 7 illustrates the cut-off k eigenvalue components at which each network is able to explain 95% of all feature variance for one eye slice of a randomly selected PD patient. For every participant

---

[47] HUANG, Gao, *et al.* "Densely connected convolutional networks". In: *Proceedings of the IEEE conference on computer vision and pattern recognition*. 2017, pp. 4700–4708.

Figure 7. Cumulative explained variance at each eigenvalue component for a randomly selected PD patient. Vertical lines indicate the cut-off k eigenvalues at which each CNN feature representation is able to explain 95% of the total channel-wise feature variability. Note that by using magnified representations, the required number of eigenvalues is slightly lower in all architectures.

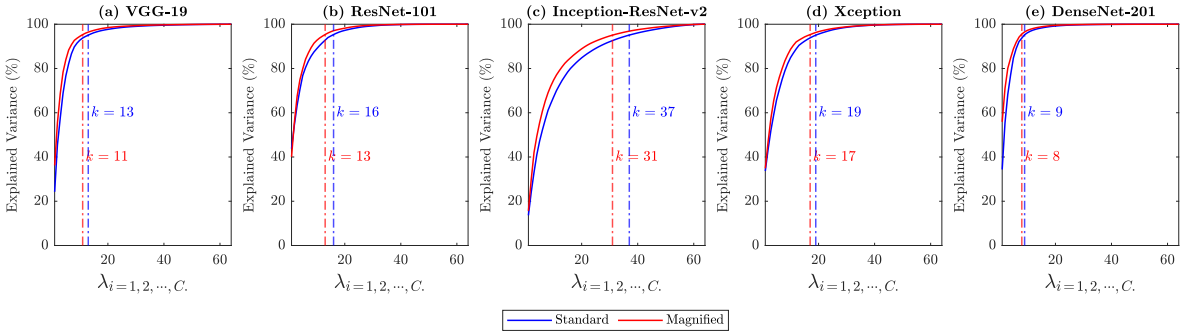

subject, the value of k was found to be approximately similar when evaluating features from a particular layer of the same CNN. This is valid for all of the considered architectures. Hence, k was automatically fixed for each CNN layer as the average cut-off eigenvalue of the population.

5. EVALUATION AND RESULTS

An extensive evaluation of the proposed approach was carried out on the symmetric case-control dataset detailed in section 4.1, that is, 130 video sequences involving 26 subjects. This evaluation was performed through a leave-one-patient-out cross-validation, i.e., sequences from one patient are left out at each iteration for testing and the remaining ones are used for training the model. Both independent and paired (concatenated) eye-fixation covariance descriptors are considered by using slice features from individual right- and left-eye sequences.

Table 1 summarizes the average performance of the studied deep architectures, over the specified first layer features (section 4.3) of eye slices from both standard and magnified sequences. Performance is measured in terms of accuracy and AUC (Area Under the ROC Curve, where ROC stands for Receiver Operating Characteristic). A total of 4 slices were used in these experiments (see Figure 3). Part (a) presents percentages of accuracy. Best results were consistently obtained for magnified sequences, with the majority of accuracy values above 90%. On the other hand, for standard sequences, the accuracy interval is mostly limited to 75–87%. Paired

Table 1. Performance evaluation over different pre-trained CNN architectures. (a) Average accuracy results by using standard and magnified videos in three descriptor configurations: right-eye covariances (R), left-eye covariances (L), and paired covariances from both eyes (R-L). (b) Area under the ROC curve in the same setting.

	(a) Accuracy (%)						**(b) AUC ROC**					
	R		**L**		**R-L**		**R**		**L**		**R-L**	
	std	**mag**	**std**	**mag**	**std**	**mag**	**std**	**mag**	**std**	**mag**	**std**	**mag**
VGG-19	86.9	86.2	77.7	**90.0**	87.7	87.7	0.916	**0.937**	0.884	**0.940**	0.911	**0.950**
ResNet-101	81.5	**92.3**	78.5	**93.1**	80.8	**95.4**	0.890	**0.975**	0.853	**0.964**	0.880	**0.984**
Inception-ResNet-v2	87.7	**92.3**	78.5	**90.8**	82.3	**93.1**	0.948	**0.981**	0.844	**0.967**	0.894	**0.976**
Xception	78.5	**88.5**	70.8	**93.8**	75.4	**93.1**	0.871	**0.925**	0.786	**0.974**	0.844	**0.968**
DenseNet-201	85.4	**87.7**	69.2	69.2	79.2	76.9	0.929	**0.954**	0.809	0.760	0.808	**0.831**

Figure 8. Best ROC curves for each of the selected CNN architectures. In all cases, the best ROC is obtained from magnified data. The corresponding non-magnified (standard) versions are also plotted for comparison.

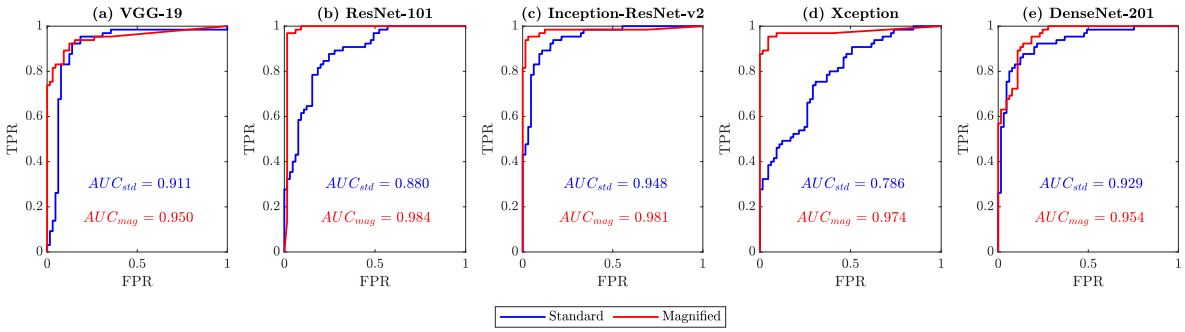

(R-L) eye-fixation covariances compared to individual (R and L) covariances only show contribution from residual networks, i.e., ResNet-101 and Inception-ResNet-v2.

ROC curves were also computed for the considered configurations. Figure 8 illustrates the best ROC per network. These plots allow to assess diagnostic performance as the ratio between True Positive Rate (TPR) and False Positive Rate (FPR) at various threshold intervals. Part (b) of Table 1 reports AUC values. Magnified AUCs present the best trade-off between TPRs and FPRs with outstanding results at distinguishing between PD patients and control subjects. For standard sequences, the obtained AUCs are still good in some configurations, e.g., 0.948 for Inception-ResNet-v2 (R descriptor). As with accuracies, the joint consideration of R and L covariances in an R-L descriptor show an improvement for the ResNet-101 architecture.

The convolutional representation of ResNet-101 architecture was the best overall setting achieving an accuracy of 95.4% and an AUC of 0.984, when using magnified sequences and R-L descriptors. The Inception-ResNet-v2 was very close to this

performance with an AUC of 0.981 (magnified sequences, R descriptor). These results imply the residual networks as best extractors of low-level slice features for the representation of fixational cues. Such assertion could be associated to the optimal gradient flow from later layers to initial filters in the residual training of ResNets, which reinforces the generalization of low-level primitives in the feature space of first representation layers. Regarding independent right- and left-eye descriptors, obtained accuracies for ResNet-101 are lower but still $>$ 90%, suggesting the capability to enrich the representation of fixational patterns by combining both eye descriptors. For the remaining networks, although there was no contribution from considering joint R-L descriptors, such combination could be done in a more elaborated way to be able to consistently exploit oculomotor patterns on both eyes. For instance, an automatic selection or weighting of relevant patterns in either right or left eye. This is of special importance in Parkinson's disease, since asymmetry on right and left sides of the body persists throughout the initial motor symptoms, and could vary differently for each patient [1].

5.1. CONFOUNDING EFFECTS

Confounding effects for gender and age variables were evaluated by computing crude and adjusted odds ratios from a logistic regression step. In such model, predictor variables x_i are linearly related with the log-odds of the outcome event y. In the case of 3 predictors, that is:

$$\log\left(\frac{p}{1-p}\right) = \beta_0 + \beta_1 x_1 + \beta_2 x_2 + \beta_3 x_3 \ , \ \ p = P(y=1) \tag{10}$$

For estimating crude and adjusted odds ratios, variables are configured as follows: y as the predicted probability of PD by the proposed methodology in this work, x_1 as the binary true label of PD diagnosis for each participant, x_2 as the gender of

Table 2. Crude odds ratios (cOR) and adjusted odds ratios (aOR) for gender and age variables. Odds ratios were computed from logistic regression coefficients, with the same classification data used for Figure 8 ROC curves.

	std			mag		
	cOR	**aOR**	***p*-value**	**cOR**	**aOR**	***p*-value**
VGG-19	6.20	6.05	0.003	7.61	7.96	0.003
ResNet-101	3.60	3.85	0.014	20.23	24.61	0.007
Inception-ResNet-v2	5.78	7.44	0.006	14.16	13.51	0.003
Xception	2.13	2.46	0.071	14.39	24.57	0.021
DenseNet-201	5.42	5.25	0.005	7.11	6.98	0.003

each participant, and x_3 as ages. For crude odds ratios (cOR), the regression coefficient β_1 is calculated without considering the effect of the other coefficients, that is $\beta_2 = \beta_3 = 0$. For adjusted odds ratios (aOR), β_1 is now calculated together with the other coefficients. The odds ratio estimation is then defined as the exponential function of β_1: e^{β_1} [48].

Table 2 presents the obtained cOR and aOR for each of the considered CNN architectures. In general, odds ratios reflect a significantly positive association between the disease diagnosis and the predicted probabilities by the proposed approach. Such association is not confounded by gender or age, indicating that these variables are not playing any part on the reported evaluation results. Also, obtained ratios from magnified data tend to be higher and more statistically significant, being the ResNet-101 architecture the best performing network.

5.2. RESNET FEATURE REPRESENTATION

Due to its good performance, the ResNet-101 architecture was selected for a more detailed analysis, exploring additional convolutional layers, measuring the impact of

[48] SZUMILAS, Magdalena. “Explaining odds ratios”. In: *Journal of the Canadian academy of child and adolescent psychiatry* 19.3 (2010), p. 227.

Table 3. Obtained accuracies for different convolutional layers of the ResNet-101 architecture.

	Layer 1		Layer 2		Layer 3	
	std	**mag**	**std**	**mag**	**std**	**mag**
R	81.5	**92.3**	77.7	84.6	70.0	83.1
L	78.5	**93.1**	76.2	89.2	77.7	82.3
R-L	80.8	**95.4**	79.9	90.0	76.9	80.8

the number of slices, and exploring the frequency magnification parameter to better highlight differences on fixational motion patterns. Firstly, layers at different levels of the architecture were evaluated to measure their representation capability. As reported in Table 3, the first layer remains as the best way to capture and represent ocular tremor patterns, as response of several primary kernels that decompose information on main frequency image bands. High-level layers nevertheless capture proper relationships of slices that eventually could be useful for additional support in complex cases, such as preliminary disease stages or under strong variations and totally-non controlled video capture. In these experiments, it also noted the relevance of the magnification stage, which yields the best results in all layers used for the proposed representation.

The impact on performance was also analyzed when using several slices in the descriptor by aggregating slices at different angles. This analysis was also implemented separately for left, right and joint eye descriptors. For reference purposes, the horizontal slice (0^o) of the video sequences was used. For experiments involving two slices, these were taken each at 90^o (horizontal and vertical planes). For four slices, a split of 45^o was considered. Six and eight slices were taken 30^o and 22.5^o apart, respectively. Figure 9 shows accuracy results over the different slice numbers, being four slices the best configuration to represent parkinsonian oculomotor patterns. Regardless of the slice number, the best performance is always obtained

Figure 9. Accuracy performance of the proposed approach by using the ResNet-101 feature representation over different slice configurations.

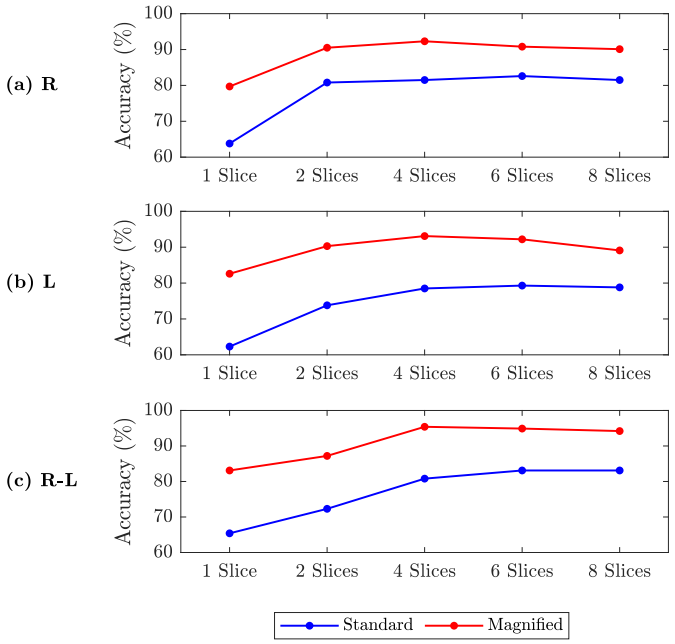

from magnified sequences. The difference in performance between standard and magnified sequences is higher when only one or two slices are utilized. The gain is almost 20% in terms of accuracy with only one slice. The use of six or eight slices slightly decreases accuracy, suggesting an overly redundant representation of analyzed patterns and favoring a more compact configuration.

Finally, an exploration of magnification frequency was carried out to evaluate its contribution w.r.t. fixation parkinsonian patterns. In this case, the temporal frequency of magnification was changed from 1 to 15 Hz. As observed in Figure 10, the proposed approach achieves equally outstanding accuracy on the specific range between 4–7 Hz. It is especially noteworthy that such frequency interval corresponds to the characteristic parkinsonian tremor frequencies observed in previous studies

Figure 10. Influence of the magnification frequency choice in the disease classification performance.

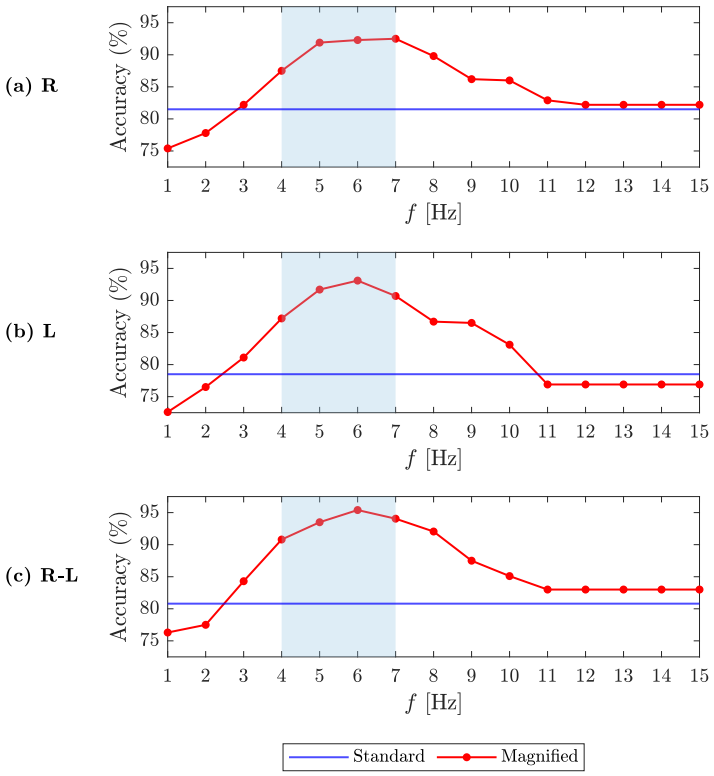

[49]. A decrease in performance is obtained on frequencies lower than 2 Hz, arguably because at this interval the signal could be related with typical head movement frequencies [17]. In such case, video magnification more likely amplifies noisy head motions. Also, for frequencies greater than 10 Hz, accuracy tends to converge to the standard behavior. This is probably explained by the absence of movements to magnify in such frequency range.

---

[49] BHATIA, Kailash P, *et al.* "Consensus Statement on the classification of tremors, from the task force on tremor of the International Parkinson and Movement Disorder Society". In: *Movement Disorders* 33.1 (2018), pp. 75–87.

6. DISCUSSION

This work presented a computerized oculomotor descriptor from eye video sequences captured during a fixation experiment. Cross-sectional slices of video-magnified sequences were used to characterize fixational micro-patterns as a parkinsonian signature signal. This characterization was done by taking advantage of the powerful generalized feature space of CNNs. In such networks, features are extracted through non-linear banks of pre-learned filters that decompose different patterns of the input images. In the problem of eye-fixation slices, convolutional features maps are an optimal representation that can better capture the fixation patterns related with the disease, since they are basically depicted as a composition of lines and edges in a spatial projection of eye motion. Feature maps are then compactly encoded as a covariance matrix descriptor that represents a summary statistic on feature space, enhancing main correlated and salient signals while removing noisy spatial information. A similar representation has been being used in texture synthesis approaches [50], by taking the correlation matrix instead of the covariance. This is because they analyze features over different network layers, resulting in different feature spaces that need to be normalized. In this work, it is addressed the extraction of a single feature space of an early CNN layer, which maintains consistent scales and therefore can benefit from the unbounded range of covariance descriptors. This feature covariance representation, when utilized for the SVM classification of PD-diagnosed and healthy subjects, yielded remarkably good performance to support the diagnostic decision.

---

[50] GATYS, Leon; ECKER, Alexander S, and BETHGE, Matthias. “Texture synthesis using convolutional neural networks”. In: *Advances in neural information processing systems*. 2015, pp. 262–270.

Video magnification, as a pre-processing step for the enhancement of fixational patterns, proves to contribute significantly in the proposed approach. Values reported in Table 1 consistently demonstrate that magnified videos lead to improved performances for the classification of PD patients. Both accuracies and AUC when using magnified videos were superior in almost all cases of different CNN architectures, different lateralities, and different number of video slices (see Figure 9). For the best configuration (ResNet-101, R-L descriptor), the utilization of magnified eye slices yielded an improvement of 18% in the classification accuracy w.r.t. standard videos (no magnification). In achieving these results, a fundamental parameter of video magnification was the estimated temporal frequency of the motion to be amplified. Best outcomes were found best in the frequency range of 4–7 Hz, which is indeed in coherence with parkinsonian ocular tremor frequencies, previously reported in the literature [16, 17]. Interestingly enough, such values also correspond to characteristic limb tremor frequencies of PD [49]. This suggests a successfully leveraging of one of the most relevant features of PD motion when classifying PD patients based solely on conventionally captured video.

A major concern when evaluating oculomotor patterns has been their correlation with head movements. For instance, Kaski et al. [21] studied the possibility that parkinsonian eye alterations during fixation could be related to vestibulo-ocular reflex responses, that is, a compensatory movement of the eyes due to head oscillations. In contrast, the herein obtained results support the findings reported by Gitchel et al. [17], who suggested that the effects of head motion are only relevant at lower frequency bands (below 1.8 Hz) w.r.t. eye motion frequencies (above 4 Hz). This is explained by Figure 10, where frequencies below 2 Hz yielded lower performances in the classification task by using magnified videos regarding standard videos. Based

on the reported results, oculomotor-related frequencies are concluded to effectively lead to performance improvements, contrary to head-related motion frequencies that in this work do not contribute to parkinsonian characterization.

Regarding other approaches in the literature that also exploit oculomotor patterns in PD classification and recognition (chapter 1), some representative works have recently evaluated other types of eye motion [25, 26, 27]. Firstly, Szymanski et al. [25] obtained accuracies above 80% in the prediction of individual UPDRS scores and Levadopa dosages when evaluating saccadic movements of PD patients. On the other hand, Zhang et al. [26] reported an AUC of 0.921 in the binary classification of PD against controls, by considering different oculomotor variables in saccadic, smooth pursuit and fixational movements. They also show the independent performance of the different eye movements, e.g., when only using fixation stability they obtained an AUC of 0.648. Finally in [27], they consider anti-saccadic kinematics and predict the UPDRS patient scores with an accuracy of 91%. All these approaches make use of VOG configurations, implying sophisticated and restrictive head-mounted apparatuses, controlled scenarios and calibration requirements. In contrast, this work was interested in evaluating oculomotor information from simpler, yet robust protocols, with direct application on clinical routine. In that sense, the obtained performance above 90% in the proposed methodology proves a promising strategy for leveraging oculomotor information that only requires conventional video cameras.

Other works have also been devoted to the development of more flexible systems with consumer-grade video devices [30, 31, 32]. These methods extract motion descriptors for a limited range of large and exploratory eye movements. In this work, the proposed pipeline for video-based oculomotor analysis uses a learned decomposition of sectional video slices, that can properly represent small local patterns

over the fixed gaze of PD patients. Such patterns include, for instance, gradients of first and second orders in oculomotor profiles that are strongly correlated with fixational micro-tremor of PD [16, 17]. As a result, this approach is able to obtain a dense kinematic representation of small fixational eye movements, which are considerably enhanced on magnified videos w.r.t. standard videos. In that way, the video magnification step represent a very useful consideration for enhancing or revealing hidden parkinsonian patterns on video.

7. CONCLUSIONS AND FUTURE WORK

In this work, a quantitative strategy to characterize ocular fixational motion was proposed as an imaging biomarker for Parkinson's disease. This approach achieved a robust eye motion modeling on conventional video sequences. For so doing, oculomotor activity of test subjects was captured, following eye fixation experiments. Acquired videos were then magnified using an optical acceleration-based framework that allowed to enhance small motility patterns. Video slice features based on primary CNN layer responses were used to classify control and PD-diagnosed patients under a supervised machine learning framework. Preliminary experiments on a study of 26 subjects yielded promising results in terms of high classification accuracy (95%) and area under the ROC curve (AUC = 0.984). The obtained results demonstrated a feasible alternative for PD assessment using ordinary and magnified videos, thus avoiding complex and sophisticated acquisition setups such as videooculography. The proposed strategy represents a potential approach to understand and quantify the association between PD and eye motility, aiming to support diagnosis and follow-up of the disease. Future work includes a deeper sensitivity analysis of computed patterns to differentiate among different stages of the disease. Further evaluation with a larger population sample is warranted, focusing efforts to recruit early-diagnosed PD patients to determine the reliability of the considered biomarker in early stages of the disease. Evaluation of other types of eye movements is also of great concern for future approaches, with aims for longitudinal studies of the patients that provide disease progression monitoring and follow-up of treatment efficacy

BIBLIOGRAPHY

ABDULHAY, Enas, *et al.* “Gait and tremor investigation using machine learning techniques for the diagnosis of Parkinson disease”. In: *Future Generation Computer Systems* 83 (2018), pp. 366–373 (cit. on p. 11).

ADHIKARI, Sam and STARK, David E. “Video-based eye tracking for neuropsychiatric assessment”. In: *Annals of the New York Academy of Sciences* 1387.1 (2017), pp. 145–152 (cit. on pp. 19, 43).

AJAY, Jerry, *et al.* “A pervasive and sensor-free deep learning system for Parkinsonian gait analysis”. In: *2018 IEEE EMBS International Conference on Biomedical & Health Informatics (BHI)*. IEEE. 2018, pp. 108–111 (cit. on p. 11).

ARCHIBALD, Neil K, *et al.* “Visual exploration in Parkinson’s disease and Parkinson’s disease dementia”. In: *Brain* 136.3 (2013), pp. 739–750 (cit. on p. 16).

BELIĆ, Minja, *et al.* “Artificial intelligence for assisting diagnostics and assessment of Parkinson’s disease–A review”. In: *Clinical neurology and neurosurgery* (2019), p. 105442 (cit. on p. 11).

BHATIA, Kailash P, *et al.* “Consensus Statement on the classification of tremors, from the task force on tremor of the International Parkinson and Movement Disorder Society”. In: *Movement Disorders* 33.1 (2018), pp. 75–87 (cit. on pp. 40, 42).

CARAMIA, Carlotta, *et al.* “IMU-Based Classification of Parkinson’s Disease From Gait: A Sensitivity Analysis on Sensor Location and Feature Selection”. In: *IEEE*

journal of biomedical and health informatics 22.6 (2018), pp. 1765–1774 (cit. on p. 11).

CHANG, Chih-Chung and LIN, Chih-Jen. “LIBSVM: A library for support vector machines”. In: *ACM Transactions on Intelligent Systems and Technology* 2 (3 2011), 27:1–27:27 (cit. on p. 27).

CHOLLET, François. “Xception: Deep learning with depthwise separable convolutions”. In: *Proceedings of the IEEE conference on computer vision and pattern recognition*. 2017, pp. 1251–1258 (cit. on p. 31).

DENG, Jia, *et al.* “ImageNet: A large-scale hierarchical image database”. In: *2009 IEEE conference on computer vision and pattern recognition*. IEEE. 2009, pp. 248–255 (cit. on p. 30).

DONAHUE, Jeff, *et al.* “Decaf: A deep convolutional activation feature for generic visual recognition”. In: *International conference on machine learning*. 2014, pp. 647–655 (cit. on p. 24).

EKKER, Merel S, *et al.* “Ocular and visual disorders in Parkinson’s disease: Common but frequently overlooked”. In: *Parkinsonism & related disorders* 40 (2017), pp. 1–10 (cit. on pp. 12, 16).

EWENCZYK, Claire, *et al.* “Antisaccades in Parkinson disease: a new marker of postural control?” In: *Neurology* 88.9 (2017), pp. 853–861 (cit. on p. 17).

FLEET, David J and JEPSON, Allan D. “Computation of component image velocity from local phase information”. In: *International journal of computer vision* 5.1 (1990), pp. 77–104 (cit. on p. 22).

FUKUSHIMA, Kikuro, *et al.* “Impaired smooth-pursuit in Parkinson’s disease: normal cue-information memory, but dysfunction of extra-retinal mechanisms for pursuit preparation and execution”. In: *Physiological reports* 3.3 (2015), e12361 (cit. on p. 17).

GATYS, Leon; ECKER, Alexander S, and BETHGE, Matthias. “Texture synthesis using convolutional neural networks”. In: *Advances in neural information processing systems*. 2015, pp. 262–270 (cit. on p. 41).

GITCHEL, George T; WETZEL, Paul A, and BARON, Mark S. “Pervasive ocular tremor in patients with Parkinson disease”. In: *Archives of neurology* 69.8 (2012), pp. 1011–1017 (cit. on pp. 12, 16, 21, 42, 44).

GITCHEL, George T, *et al.* “Experimental support that ocular tremor in Parkinson’s disease does not originate from head movement”. In: *Parkinsonism & related disorders* 20.7 (2014), pp. 743–747 (cit. on pp. 13, 16, 21, 40, 42, 44).

GOETZ, Christopher G, *et al.* “Movement Disorder Society Task Force report on the Hoehn and Yahr staging scale: status and recommendations the Movement Disorder Society Task Force on rating scales for Parkinson’s disease”. In: *Movement disorders* 19.9 (2004), pp. 1020–1028 (cit. on p. 28).

GOLDBERG, M. E and WALKER, M. F. “The control of gaze”. In: *Principles of Neural Science*. Ed. by Eric R. KANDEL, *et al.* 5th. USA: New York: McGraw-Hill, 2013, pp. 894–916 (cit. on pp. 12, 16).

GORGES, Martin, *et al.* “The association between alterations of eye movement control and cerebral intrinsic functional connectivity in Parkinson’s disease”. In: *Brain imaging and behavior* 10.1 (2016), pp. 79–91 (cit. on pp. 12, 17).

HANUŠKA, Jaromír, *et al.* “Fast vergence eye movements are disrupted in Parkinson’s disease: A video-oculography study”. In: *Parkinsonism & related disorders* 21.7 (2015), pp. 797–799 (cit. on p. 17).

HE, Kaiming, *et al.* “Deep residual learning for image recognition”. In: *Proceedings of the IEEE conference on computer vision and pattern recognition*. 2016, pp. 770–778 (cit. on p. 31).

HU, Kun, *et al.* “Vision-based freezing of gait detection with anatomic patch based representation”. In: *Asian Conference on Computer Vision*. Springer. 2018, pp. 564–576 (cit. on p. 11).

HUANG, Gao, *et al.* “Densely connected convolutional networks”. In: *Proceedings of the IEEE conference on computer vision and pattern recognition*. 2017, pp. 4700–4708 (cit. on p. 32).

IRANZO, Alex; SANTAMARIA, Joan, and TOLOSA, Eduardo. “Idiopathic rapid eye movement sleep behaviour disorder: diagnosis, management, and the need for neuroprotective interventions”. In: *The Lancet Neurology* 15.4 (2016), pp. 405–419 (cit. on p. 12).

JANKOVIC, Joseph. “Parkinson’s disease: clinical features and diagnosis”. In: *Journal of neurology, neurosurgery & psychiatry* 79.4 (2008), pp. 368–376 (cit. on p. 10).

KASKI, Diego, *et al.* “Ocular tremor in Parkinson’s disease is due to head oscillation”. In: *Movement Disorders* 28.4 (2013), pp. 534–537 (cit. on pp. 17, 42).

KHOSLA, Ajit and KIM, Dongsoo. *Optical Imaging Devices: New Technologies and Applications*. CRC Press, 2015 (cit. on p. 18).

KUBIS, Anna; SZYMAŃSKI, Artur, and PRZYBYSZEWSKI, Andrzej W. “Fuzzy Rough sets theory applied to parameters of eye movements can help to predict effects of different treatments in Parkinson’s patients”. In: *International Conference on Pattern Recognition and Machine Intelligence*. Springer. 2015, pp. 325–334 (cit. on p. 18).

LAI, Hsin-Yu, *et al.* “Enabling Saccade Latency Measurements with Consumer-Grade Cameras”. In: *2018 25th IEEE International Conference on Image Processing (ICIP)*. IEEE. 2018, pp. 3169–3173 (cit. on pp. 19, 43).

LAL, Vivek and TRUONG, Daniel. “Eye movement abnormalities in movement disorders”. In: *Clinical Parkinsonism Related Disorders* 1 (2019), pp. 54 –63 (cit. on p. 16).

LARRAZABAL, AJ; CENA, CE García, and MARTÍNEZ, CE. “Video-oculography eye tracking towards clinical applications: A review”. In: *Computers in biology and medicine* 108 (2019), pp. 57 –66 (cit. on p. 13).

POEWE, Werner, *et al.* “Parkinson disease”. In: *Nature reviews Disease primers* 3 (2017), p. 17013 (cit. on pp. 10, 11, 36).

PORTILLA, Javier and SIMONCELLI, Eero P. “A parametric texture model based on joint statistics of complex wavelet coefficients”. In: *International journal of computer vision* 40.1 (2000), pp. 49–70 (cit. on p. 22).

RIZZO, Giovanni, *et al.* “Accuracy of clinical diagnosis of Parkinson disease A systematic review and meta-analysis”. In: *Neurology* 86.6 (2016), pp. 566–576 (cit. on p. 10).

SALAT, David, *et al.* “Challenges of modifying disease progression in prediagnostic Parkinson’s disease”. In: *The Lancet Neurology* 15.6 (2016), pp. 637–648 (cit. on p. 11).

SHARIF RAZAVIAN, Ali, *et al.* “CNN features off-the-shelf: an astounding baseline for recognition”. In: *Proceedings of the IEEE conference on computer vision and pattern recognition workshops*. 2014, pp. 806–813 (cit. on p. 24).

SIMONYAN, Karen and ZISSERMAN, Andrew. “Very deep convolutional networks for large-scale image recognition”. In: *arXiv preprint arXiv:1409.1556* (2014) (cit. on p. 31).

SLEDZIANOWSKI, Albert, *et al.* “Measurements of Antisaccades Parameters Can Improve the Prediction of Parkinson’s Disease Progression”. In: *Asian Conference on Intelligent Information and Database Systems*. Springer. 2019, pp. 602–614 (cit. on pp. 18, 43).

SZEGEDY, Christian, *et al.* “Inception-v4, inception-resnet and the impact of residual connections on learning”. In: *Thirty-First AAAI Conference on Artificial Intelligence*. 2017 (cit. on p. 31).

SZUMILAS, Magdalena. “Explaining odds ratios”. In: *Journal of the Canadian academy of child and adolescent psychiatry* 19.3 (2010), p. 227 (cit. on p. 37).

SZYMAŃSKI, Artur, *et al.* “Building Intelligent Classifiers for Doctor-Independent Parkinson’s Disease Treatments”. In: *Conference of Information Technologies in Biomedicine*. Springer. 2016, pp. 267–276 (cit. on pp. 18, 43).

TRUJILLO, David, *et al.* “A characterization of Parkinson’s disease by describing the visual field motion during gait”. In: *11th International Symposium on Medical Information Processing and Analysis*. Vol. 9681. SPIE (2015) (cit. on pp. 19, 43).

TURCANO, Pierpaolo, *et al.* “Early ophthalmologic features of Parkinson’s disease: a review of preceding clinical and diagnostic markers”. In: *Journal of neurology* (2018), pp. 1–9 (cit. on pp. 12, 16).

VENUTO, Charles S, *et al.* “A review of disease progression models of Parkinson’s disease and applications in clinical trials”. In: *Movement Disorders* 31.7 (2016), pp. 947–956 (cit. on p. 10).

WADHWA, Neal, *et al.* “Phase-based video motion processing”. In: *ACM Transactions on Graphics (TOG)* 32.4 (2013), p. 80 (cit. on p. 22).

WU, Hao-Yu, *et al.* “Eulerian Video Magnification for Revealing Subtle Changes in the World”. In: *ACM Transactions on Graphics (Proc. SIGGRAPH 2012)* 31.4 (2012) (cit. on p. 22).

ZHANG, Yichao; PINTEA, Silvia L., and VAN GEMERT, Jan C. “Video Acceleration Magnification”. In: *Computer Vision and Pattern Recognition*. 2017 (cit. on p. 21).

ZHANG, Yu, *et al.* “Oculomotor Performances Are Associated With Motor and Non-motor Symptoms in Parkinson’s Disease”. In: *Frontiers in neurology* 9 (2018), p. 960 (cit. on pp. 18, 43).

ANEXOS

Anexo A. Academic Products

Journals

- I. Salazar, S. Pertuz, W. Contreras, F. Martínez. "A convolutional oculomotor representation to model parkinsonian fixational patterns from magnified videos". Pattern Analysis and Applications. Springer London.
  Status: Submitted.

Conference papers

- I. Salazar, S. Pertuz, W. Contreras, F. Martínez. "Parkinsonian ocular fixation patterns from magnified videos and CNN features". 24th Iberoamerican Congress on Pattern Recognition (CIARP 2019). In Lecture Notes in Computer Science, vol. 11896. 22 October 2019, Springer Cham. DOI: 10.1007/978-3-030-33904-3_70.

Collaborations

- B. Valenzuela, I. Salazar, F. Martínez. "Lagrangian center of mass (CoMt) magnification to stand out main parkinsonian gait events". XXII Symposium on Image, Signal Processing and Artificial Vision (STSIVA 2019). In IEEE Xplore Digital Library. 06 June 2019, IEEE. DOI: 10.1109/STSIVA.2019.8730254.

- S. Contreras, I. Salazar, F. Martínez. "Parkinsonian hand tremor characterization from magnified video sequences". 14th International Symposium on Medical Information Processing and Analysis (SIPAIM 2018). In Proceedings of SPIE - The International Society for Optics and Photonics, vol. 10975. 21 December 2018, SPIE. DOI: 10.1117/12.2512109.

Anexo B. Video Stimuli for Oculomotor Recording

This anexo summarizes in Figure 11 the utilized stimuli sequences for the video dataset of eye movements proposed in this research work. Three relevant visual tasks were considered in three eye-recording rounds. A brief sound signal is emitted between each task to indicate the beginning of a new oculomotor type in the recorded eye videos. A description of the visual tasks is presented below:

- **Fixation:** For the three recordings, each participant stares at the fixed dot stimulus for 10 seconds, preceded or followed by another type of oculomotor task.
- **Smooth Pursuit:** For the first recording, each participant follows the moving dot stimulus in a circular trajectory with duration of 10 seconds. For the second recording, the dot now moves from right (1) to left (2), and then from up (3) to down (4). Total trajectory duration is 15 seconds. For the third recording, a similar trajectory is followed but in a diagonal pattern, also of 15 seconds length.
- **Random Saccades:** For the three recordings, each participant executes a saccade every 2 seconds to change the fixation target. The dot stimulus suddenly changes position 10 times, following a random pattern on the screen. Thus, 10 saccades are expected in a period of 20 seconds.

The developed approach was delimited to the evaluation of ocular fixation. Therefore, fixation periods were trimmed on the temporal axis. A spatial crop was also manually carried out to obtain concise and compact eye sequences. Figure 12 shows some of the ready-to-process eye sequences of PD-diagnosed patients. The dataset is currently in process to be released with the three oculomotor categories for further

Figure 11. Stimuli sequences that were generated for the recording of eye movements. There were generated 3 different sequences for 3 eye-recording rounds per person, with a total of 5 fixation periods. These fixation samples were individually cropped and thus considered for the evaluation of the proposed methodology in this work.

(a) Stimuli sequence for the first recording (50 seconds).

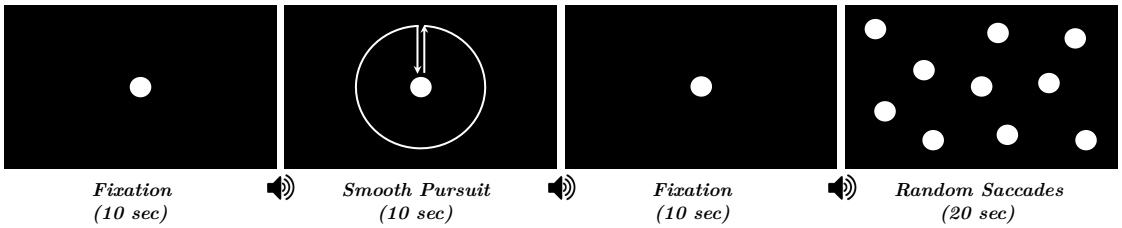

(b) Stimuli sequence for the second recording (45 seconds).

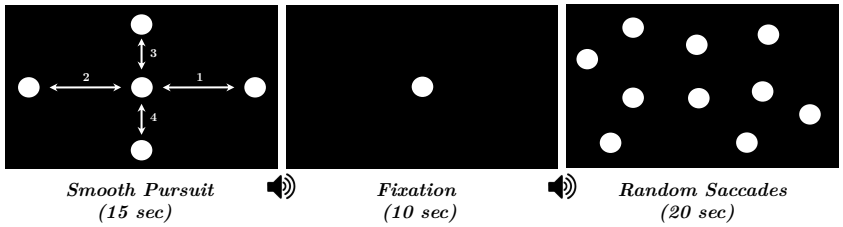

(c) Stimuli sequence for the third recording (55 seconds).

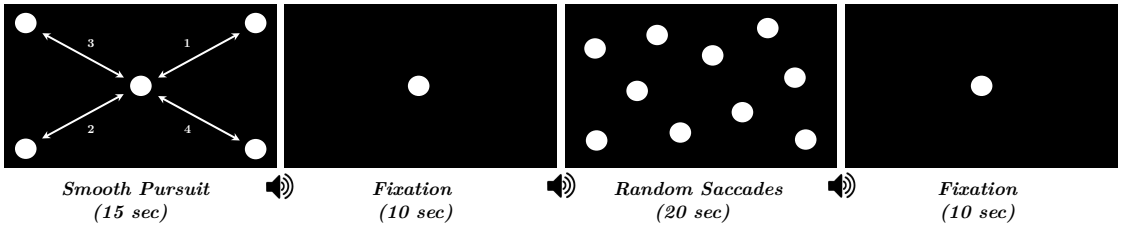

academic research, and it will be available at [51].

[51] http://bivl2ab.uis.edu.co/

Figure 12. Pre-processed dataset samples.

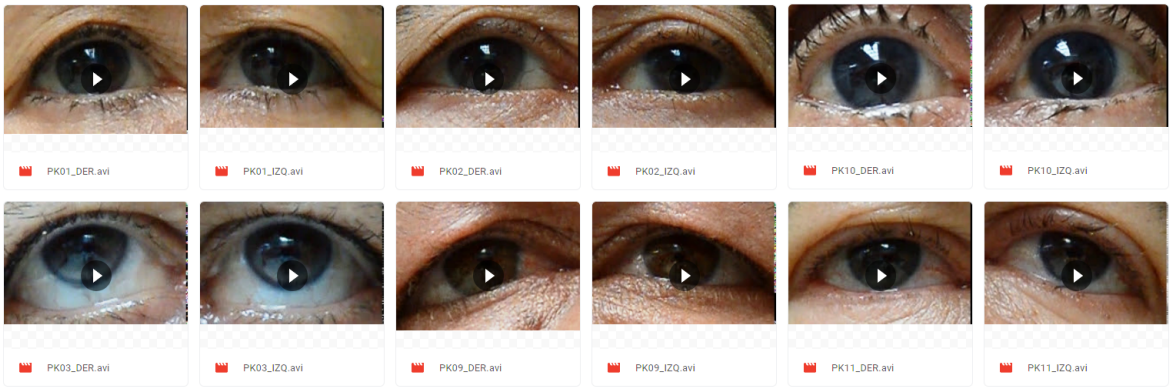

Anexo C. Informed Consent

Universidad Industrial de Santander	**CONSENTIMIENTO INFORMADO**	**Código:**
		Versión: 03 31/07/2019
		Página: 1 de 5

ESCUELA DE INGENIERÍA DE SISTEMAS
UNIVERSIDAD INDUSTRIAL DE SANTANDER

Proyecto: Amplificación visual de signos óculo-motores para el reconocimiento de patrones parkinsonianos.

Responsable(s):

- Isail Salazar Acosta
  Estudiante de Maestría en Ingeniería de Sistemas e Informática
  Universidad Industrial de Santander

- Fabio Martínez Carrillo
  Docente Planta, Escuela de Ingeniería de Sistemas e Informática
  Universidad Industrial de Santander

Con base en los reglamentos establecidos en la Resolución N° 8430 del 4 de octubre de 1993 por la cual se establecen las normas para la investigación en salud en Colombia, específicamente en el Artículo 15, mediante este documento de consentimiento informado usted deberá conocer acerca de esta investigación y aceptar participar en ella si lo considera conveniente. De esta manera, se le invita formalmente a participar teniendo en cuenta los siguientes criterios de inclusión:

- Ser mayor de edad.
- Tener la capacidad para sentarse en una postura cómoda y relajada que le permita visualizar un punto proyectado en pantalla.
- No presentar ninguna enfermedad que afecte los movimientos de sus ojos, a excepción de la enfermedad de Parkinson.

En vista del cumplimiento de los criterios anteriores, por favor seleccione una de las siguientes opciones según su diagnóstico actual :

___ **Persona control**: Es aquella persona que no presenta ninguna dificultad motora, implicando que no ha sido diagnosticada de ninguna enfermedad que afecte su movimiento natural.

___ **Paciente parkinsoniano**: Es aquella persona que ha sido diagnosticada con la enfermedad de Parkinson.

Tenga en cuenta que su participación en este proyecto es ***absolutamente voluntaria***. Por favor lea con cuidado el documento y realice todas las preguntas que desee hasta su total comprensión.

JUSTIFICACIÓN

Usted está invitado a participar en este estudio sobre movimientos oculares en distintas actividades de fijación y seguimiento visual de objetivos en pantalla. Los movimientos se esperan analizar en video, registrados de manera natural mediante una cámara convencional. La finalidad principal es desarrollar una herramienta tecnológica que facilite la detección y el monitoreo de anormalidades en los movimientos de los ojos, con la premisa de que estas anormalidades representan un potencial

indicador en el diagnóstico en la enfermedad de Parkinson. Con los resultados a obtener, se espera entonces contribuir en el soporte diagnóstico de la enfermedad, así como también estudiar su evolución en tratamiento particulares. El análisis de los movimientos registrados se realizará teniendo en cuenta el diagnóstico previo desarrollado por un experto clínico, por lo tanto, en este estudio no se esperan obtener diagnósticos diferentes a los previamente establecidos.

OBJETIVO

Diseñar una herramienta tecnológica que permita apoyar procedimientos clínicos en cuanto a la identificación y análisis de los movimientos de los ojos que puedan estar asociados a la enfermedad de Parkinson, mediante el procesamiento de los videos registrados gracias a su participación.

DESCRIPCIÓN

La siguiente descripción del procedimiento aplica, indistintamente, tanto para las personas control como para los pacientes diagnosticados con enfermedad de Parkinson. Esto debido a que el estudio considera que los datos han sido capturados bajo las mismas condiciones en ambas poblaciones, en miras de una adecuada evaluación estadística. Esta convocatoria se limita a la población residente en la ciudad de Bucaramanga, tratada como etapa preliminar de futuras investigaciones más amplias.

Para la realización del estudio, se dispone de los espacios de dos instituciones locales: el **Centro Vida Años Maravillosos**, ubicado en la Diagonal 14 #56-02 Barrio Real de Minas, y la **Fundación Adulto Mayor y Parkinson Santander (FAMPAS)**, ubicada en la Calle 54 #23-14 Barrio Sotomayor. Estas instituciones cuentan con profesionales de la salud que laboran y dirigen distintas actividades en el ejercer habitual de las mismas. Usted será citado a la institución más cercana, o a la que frecuente comúnmente.

A cada participante, en presencia de su acompañante, familiar o representante legal, se le entregará este documento para su lectura. Si decide participar, podrá proceder a firmarlo. Seguidamente se registrarán sus datos personales. La filmación de videos tomará un tiempo aproximado de 10 minutos. En caso de usar gafas, se le pedirá removerlas momentáneamente durante la prueba, asegurando primero que usted pueda visualizar sin esfuerzo o agotamiento visual el objetivo proyectado en pantalla. De no ser así, se podrá igualmente realizar la captura utilizando sus gafas. Ante la cámara, usted expondrá sus ojos mirando hacia un televisor que le presentará un estímulo visual, como se muestra en la Figura 1.

Figura 1. Escenario de captura. El participante se sentará de la manera que considera más cómoda para visualizar y seguir un punto de alto contraste proyectado en un televisor.

Al participar en este estudio, usted no recibirá ningún tipo de subvención económica o material, ni deberá aportar herramienta alguna para la intervención. Al finalizar la investigación, usted podrá recibir los resultados obtenidos en forma de un reporte que describirá diferentes aspectos sobre los movimientos de sus ojos. Este material será presentado a usted por el investigador principal en la respectiva institución donde se le realizó la grabación, junto con la explicación de las interpretaciones técnicas y clínicas, soportadas por los profesionales de salud que allí laboran.

Las inquietudes adicionales que puedan surgir en relación con el desarrollo e implicaciones de la investigación podrán ser aclaradas por el investigador Fabio Martínez Carrillo, profesor de la Escuela de Ingeniería de Sistemas e Informática, a quien puede contactar mediante el teléfono celular 3103054041, o a través del correo electrónico *famarcar@saber.uis.edu.co*; o directamente en su oficina en la Universidad Industrial de Santander (sede principal), ubicada en la Cra. 27 # 9, Edificio de Laboratorios Pesados, oficina 231, con número de teléfono 6344000 extensión 2110.

RIESGOS

De acuerdo con el Artículo 11 de la Resolución No. 8430 del 4 de octubre de 1993, esta investigación se considera de riesgo mínimo dado que el estudio únicamente emplea el registro de datos a través de un procedimiento común de captura de videos por medio de cámaras ordinarias. De tal forma, ninguno de los métodos utilizados es invasivo o penetra la piel. Si durante la captura usted experimenta cualquier tipo de malestar, esta se suspenderá de inmediato y se le ubicará en estado de reposo. De requerirse una valoración médica inmediata, se le remitirá al servicio de urgencias del Hospital Universitario de Santander o al servicio de la entidad en el que se encuentre afiliado al sistema de seguridad social. Durante este proceso, usted será acompañado por el investigador principal.

DERECHO A RETIRARSE

Su participación en este estudio es autónoma y voluntaria, en donde podrá actuar acorde a sus principios personales. Si usted decide no participar, no implicará sanción alguna. Además, usted cuenta con el derecho a negarse a responder a preguntas concretas si así lo desea. También puede optar por retirarse en cualquier momento y toda su información será descartada y eliminada.

CONFIDENCIALIDAD

La información de cada participante es de carácter absolutamente confidencial, de manera que solamente usted y el investigador principal tendrán acceso a ellos. Su uso será exclusivamente académico. Los registros con su información serán archivados por el investigador principal y a cada uno se le asignará un número con el cual se identificará y se codificará para su ingreso a la base de datos. Su nombre o datos personales no serán expuestos de ningún modo. Los resultados obtenidos de la investigación podrán ser divulgados en revistas o eventos científicos asegurando que toda su información sea debidamente anonimizada.

A no ser que usted otorgue una autorización específica según la ley, sus resultados personales no estarán disponibles para terceros como empleadores, organizaciones gubernamentales, compañías de seguros u otras instituciones educativas. Esto también será aplicado a los miembros de su familia. No obstante, con el objetivo de garantizar una gestión adecuada de los datos, un miembro del Comité de Ética de la Universidad Industrial de Santander podrá consultarlos y verificar su registro.

AUTORIZACIÓN PARA EL USO DE LA INFORMACIÓN EN ESTUDIOS FUTUROS

Dentro del equipo de investigación al que pertenecen los investigadores responsables (Grupo de Investigación BIVL2ab - *Biomedical Imaging, Vision, and Learning Laboratory*) de la Universidad Industrial de Santander, se espera seguir utilizando la información registrada en este estudio para el desarrollo de estudios futuros y derivados. Por lo tanto, al firmar este consentimiento usted puede autorizar al investigador principal a ceder su información a otros investigadores de su equipo de investigación, con previa aprobación del Comité de Ética de la Universidad Industrial de Santander para realizar los estudios mencionados. Por favor marcar con una X si autoriza o no autoriza, y firmar en caso de si autorizar.

Si autorizo _____

No autorizo _____

_____
Firma de la autorización

Huella digital
(en los casos que se amerite)

Yo_____, identificado con _____ N°_____ de _____, al firmar este consentimiento el día _____, acepto participar de manera voluntaria en el presente estudio y autorizo la grabación de mis videos y el uso de mis datos individuales para los análisis requeridos. He leído y entendido la información registrada en este documento y mis dudas fueron aclaradas. Por otro lado, se me ha garantizado la confidencialidad en el manejo de toda la información recolectada, teniendo en cuenta que los resultados del procesamiento de dicha información podrán ser divulgados con fines científicos, mediante presentaciones en congresos o publicaciones en revistas científicas, con la debida protección de mi identidad.

_____ _____
Nombre del Participante Firma
Edad: _____

Huella digital (en los casos que se amerite) :

_____ _____
Nombre del Profesional de Salud (Testigo 1) Firma
Cargo: _____
Teléfono: _____

_____ _____
Nombre del Testigo 2 Firma
Relación que guarda con el participante: _____
Teléfono: _____

_____ _____
Nombre del Investigador Principal Firma
C.C.: _____
Teléfono: _____
E-mail: _____

Contacto Comité de Ética: Para preguntas o aclaraciones acerca de los aspectos éticos de esta investigación pueden comunicarse con cualquiera de los miembros del Comité de Ética para la Investigación Científica de la Universidad Industrial de Santander (CEINCI-UIS), mediante el teléfono 6344000 Extensión 3808 ó al correo electrónico *comitedetica@uis.edu.co*.